

• 专题研究:肿瘤 •

超声黏弹性成像瘤周参数对BI-RADS 4类乳腺结节良恶性的预测价值

周锋盛^{1,2}, 袁琳¹, 浦浙宁³, 吴越¹, 张雨¹, 杨树东⁴, 秦安⁵, 张平洋^{2*}

¹南京医科大学附属无锡人民医院(南京医科大学无锡医学中心)超声医学科, 江苏 无锡 214023; ²南京医科大学附属南京医院心血管超声科, 江苏 南京 210006; ³南京医科大学附属无锡人民医院(南京医科大学无锡医学中心)检验科, ⁴病理科, ⁵乳腺外科, 江苏 无锡 214023

[摘要] 目的: 探讨黏弹性成像(viscoelasticity, VE)对乳腺影像报告和数据系统(breast imaging reporting and data system, BI-RADS)4类乳腺结节良恶性的预测价值。方法: 回顾性分析2024年2月—2025年3月在南京医科大学附属无锡人民医院就诊的常规超声诊断BI-RADS 4类乳腺结节患者102例(共105个结节), 应用VE和剪切波弹性成像(shear-wave elastography, SWE)测量乳腺结节超声参数, 通过系统测量工具“Shell”, 以1.0 mm为间隔, 手动调整壳体厚度(n)为1.0~5.0 mm, 获取瘤周VE、SWE超声参数, 比较两组超声参数的差异。绘制受试者工作特征(receiver operating characteristic, ROC)曲线分析VE、SWE超声参数及常规超声BI-RADS分类单独或联合预测BI-RADS 4类乳腺结节性质的诊断效能。结果: 入选BI-RADS 4类乳腺结节105个, 根据病理结果分为良性组58个, 恶性组47个。两组SWE超声参数以Shell2.0剪切波弹性模量参数最大值(E_{max})诊断价值最高, 当截断值为89.48 kPa时, 其预测BI-RADS 4类乳腺结节良恶性的曲线下面积(area under the curve, AUC)为0.709, 灵敏度为53.20%, 特异度为84.50%; 两组VE超声参数以Shell3.0黏弹性参数最大值(V_{max})诊断价值最高, 当截断值为5.77 Pa·s时, 其预测BI-RADS 4类乳腺结节良恶性的AUC为0.750, 灵敏度为70.21%, 特异度为72.41%; 将Shell2.0 E_{max}和Shell3.0 V_{max}与BI-RADS分类联合, 预测BI-RADS 4类乳腺结节良恶性的AUC值提升至0.941, 灵敏度高达93.60%, 特异度也达到93.10%, 差异具有统计学意义($P < 0.05$)。结论: VE瘤周超声参数预测BI-RADS 4类乳腺结节良恶性具有较高的诊断价值, VE与SWE技术联合常规超声BI-RADS分类对BI-RADS 4类乳腺结节良恶性的诊断效能最佳。

[关键词] 乳腺结节; 黏弹性成像; 超声; BI-RADS 4类

[中图分类号] R730.41

[文献标志码] A

[文章编号] 1007-4368(2025)11-1563-09

doi: 10.7655/NYDXBNSN250876

The predictive value of ultrasound viscoelastic imaging peritumoral parameters for benign and malignant BI-RADS 4 breast nodules

ZHOU Fengsheng^{1,2}, YUAN Lin¹, PU Zhening³, WU Yue¹, ZHANG Yu¹, YANG Shudong⁴, QIN An⁵, ZHANG Pingyang^{2*}

¹Department of Ultrasound Medicine, the Affiliated Wuxi People's Hospital of Nanjing Medical University (Wuxi Medical Center, Nanjing Medical University), Wuxi 214023; ²Department of Cardiovascular Ultrasound, the Affiliated Nanjing Hospital of Nanjing Medical University, Nanjing 210006; ³Department of Laboratory Medicine, ⁴Department of Pathology, ⁵Department of Breast Surgery, the Affiliated Wuxi People's Hospital of Nanjing Medical University (Wuxi Medical Center, Nanjing Medical University), Wuxi 214023, China

[Abstract] **Objective:** To explore the predictive values of viscoelasticity (VE) for benign and malignant breast imaging reporting and data system (BI-RADS) 4 breast nodules. **Methods:** A total of 102 patients (105 nodules) with BI-RADS 4 breast nodules diagnosed by conventional ultrasound in Wuxi People's Hospital Affiliated to Nanjing Medical University from February 2024 to March 2025 were retrospectively analyzed. VE and shear-wave elastography (SWE) were used to measure ultrasound parameters. Through the system measurement tool "Shell", the Shell thickness (n) was manually adjusted from 1.0 to 5.0 mm at an interval of 1.0 mm to obtain the

[基金项目] 南京医科大学无锡医学中心队列与临床研究计划(WMCC202304)

*通信作者 (Corresponding author), E-mail: zhpy28@hotmail.com (ORCID: 0000-0001-7605-3916)

peritumoral ultrasound parameters, and the differences of ultrasonic parameters between the two groups were compared. The receiver operating characteristic (ROC) curve was drawn to analyze the diagnostic efficacy of VE, SWE ultrasound parameters and conventional ultrasound BI-RADS classification alone or combined to predict the nature of BI-RADS 4 breast nodules. **Results:** A total of 105 BI-RADS 4 breast nodules were selected and divided into the benign group ($n=58$) and the malignant group ($n=47$) according to the pathological results. The diagnostic value of Shell2.0 maximum elastic modulus value (E_{max}) was the highest in the two groups of SWE ultrasound parameters. When the cutoff value was 89.48 kPa, its area under the ROC curve (AUC) for predicting the benign and malignant of BI-RADS 4 breast nodules was 0.709, the sensitivity was 53.20%, and the specificity was 84.50%. The diagnostic value of Shell3.0 maximum viscosity value (V_{max}) was the highest in the two groups of VE ultrasound parameters. When the cutoff value was 5.77 Pa·s, its AUC for predicting the benign and malignant of BI-RADS 4 breast nodules was 0.750, the sensitivity was 70.21%, and the specificity was 72.41%. When Shell2.0 E_{max} and Shell3.0 V_{max} were combined with BI-RADS classification to predict the benign and malignant of BI-RADS 4 breast nodules, the AUC value increased to 0.941, with a sensitivity of 93.60% and a specificity of 93.10%, and the difference was statistically significant ($P < 0.05$). **Conclusion:** VE peritumoral parameters alone have high diagnostic value in predicting the benign and malignant of BI-RADS 4 breast nodules. VE, SWE technology combined with conventional ultrasound BI-RADS classification has the best diagnostic efficiency for the benign and malignant of BI-RADS 4 breast nodules.

[Key words] breast nodule; viscoelastic imaging; ultrasound; BI-RADS 4 class

[J Nanjing Med Univ, 2025, 45(11): 1563-1571]

国际癌症研究机构2022年发布报告显示乳腺癌约占全球癌症总数的11.6%，已成为全球女性群体中最为常见的癌症类型^[1]，对女性生理健康、心理健康及生活质量造成严重且持续的负面影响。美国放射学会发布的第5版乳腺影像报告和数据系统 (breast imaging reporting and data system, BI-RADS) 分类指南被证实能有效评估乳腺结节的性质及恶性风险范围^[2]，其中BI-RADS 4类乳腺结节恶性程度2%~95%，范围跨度过大，影响常规超声对乳腺结节诊疗方案的制定，因此提高BI-RADS 4类乳腺结节的诊断准确度对于指导临床治疗及改善患者预后至关重要。欧洲医学和生物学超声学会联合会指南提出剪切波弹性成像 (shear-wave elastography, SWE) 是一种具备实时定量评估软组织硬度的弹性成像技术^[3]。多项研究表明，SWE是常规超声检查诊断乳腺肿块良恶性的重要补充^[4-6]。但SWE技术以乳腺、甲状腺等组织为纯弹性介质作为假设条件，而乳腺具有一定的黏弹性反应^[7-8]，因此SWE对乳腺病变硬度的评估存在一定误差。黏弹性成像 (viscoelasticity, VE) 技术通过加入黏性物理参数，弥补了SWE技术的不足，有望成为辅助诊断乳腺病变的新技术。本研究旨在探讨VE、SWE技术单独或与联合应用鉴别BI-RADS 4类乳腺结节良恶性的临床价值，为乳腺癌的早期诊断提供重要依据。

1 对象和方法

1.1 对象

回顾性选取2024年2月—2025年3月在南京

医科大学附属无锡人民医院就诊的乳腺结节患者102例 (共计105个结节)。纳入标准：①术前常规超声检查诊断BI-RADS 4类乳腺结节；②术前均行SWE和VE超声检查；③年龄 ≥ 18 岁；④均有手术或超声穿刺活检明确病理结果；⑤术前未进行任何治疗。排除标准：①乳腺异物，如假体等；②乳腺结节伴粗大钙化；③妊娠期或哺乳期女性乳腺；④超声图像质量不佳或临床资料不全；⑤患有其他严重精神病或器质性疾病。本研究经本院伦理委员会批准 (批号：2022LLPJ-IIQT-007)，患者均签署知情同意书。

1.2 方法

1.2.1 超声检查

采用迈瑞Resona A20S超声诊断仪，高频线阵探头LM18-5WU，探头频率为5~18 Hz，进行常规超声、SWE及VE超声检查。所有超声检查均由两名经验丰富的主任医师独立完成，且所有关键参数均经过3次重复测量并取平均值以确保数据的准确性。

1.2.2 常规超声BI-RADS 4类乳腺结节入组标准

患者取仰卧位，将手举过头顶，充分暴露乳房区域，对双侧乳腺进行全面连续动态扫查，明确乳腺病变的大小、形态、边缘特征、回声模式、钙化、后方特征及血流情况等超声特征。根据2013年第5版BI-RADS分类标准^[9]将4类乳腺结节分为4A、4B、4C亚类。本研究根据常规超声结果初步将BI-RADS 4A类的结节判定为良性，4B、4C类结节判定为恶性。

1.2.3 SWE及VE超声检查

选取二维超声清晰显示病灶最大直径及周围

组织的切面,感兴趣区(region of interest, ROI)要包含整个乳房结节和周围至少5 cm的乳腺组织,要求患者屏住呼吸,医生尽可能小压力稳定探头,直到运动稳定性指数(motion stability index, M-STB index)五星显示在图像的右上方,然后激活弹性成像功能,将乳腺结节二维超声图像、SWE图像、VE图像及应变比图像分别显示为四视图模式。人工手动在二维超声图像上勾勒出病变轮廓,使用系统内置软件自动获取基于Voigt模型的参数,包括黏弹性参数平均值(Vmean)、最大值(Vmax)、最小值(Vmin)、标准差(Vsd)和剪切波弹性模量参数平均值(Emean)、最大值(Emax)、最小值(Emin)、标准差(Esd),通过系统测量工具“Shell”自动获取乳腺病变瘤周区域的VE及SWE超声参数,手动调整壳体厚度(n),并以1.0 mm为间隔差值,向瘤体外部逐层构建Shell环,直至5.0 mm。乳腺病变瘤周区域获得VE超声参数Shelln(Vmax、Vmean、Vmin、Vsd)和SWE超声参数Shelln(Emax、Emean、Emin、Esd),其中n代表壳体厚度。SWE值和VE值分别用kPa和Pa·s表示。记录乳腺病灶的最大值,以及Shell1.0至Shell5.0的VE超声参数(包括Vmax、Vmean、Vmin、Vsd)和SWE超声参数(包括Emax、Emean、Emin、Esd)。

1.3 统计学方法

数据分析使用统计学软件SPSS 26.0和GraphPad Prism 9.0。分类变量以例数(百分比)[$n(\%)$]表示,采用 χ^2 检验。连续变量符合正态分布以均数±标准差($\bar{x} \pm s$)表示,采用独立样本 t 检验;不符合正态分布以中位数(四分位数)[$M(P_{25}, P_{75})$]表示,采用Mann-Whitney U 检验。绘制受试者工作特征(receiver operating characteristic, ROC)曲线分析SWE、VE超声参数及常规超声BI-RADS分类单独或联合应用预测BI-RADS 4类乳腺结节良恶性的诊断价值,曲线下面积(area under the curve, AUC)差异采用DeLong检验。 $P < 0.05$ 为差异有统计学意义。

2 结果

2.1 临床病理特征

入选BI-RADS 4类乳腺结节患者102例(105个结节),均为女性,年龄(46.88 ± 14.05)岁(21~81岁)。根据手术或穿刺活检病理结果分为良性组55例(58个结节),包括纤维腺瘤22个,腺病8个,乳腺增生症18个,乳腺炎性病变2个,导管内乳头状瘤8个;恶性组47例(47个结节),包括浸润性导管癌33个,导管内原位癌7个,浸润性小叶癌3个,黏

液癌1个,髓样癌1个,乳头状癌2个。良性组年龄(40.55 ± 12.04)岁,恶性组年龄(54.70 ± 12.40)岁,差异有统计学意义($t=5.910, P < 0.001$)。良性组病灶最大值(17.00 ± 7.04)mm,恶性组病灶最大值(20.53 ± 7.50)mm,差异无统计学意义($P > 0.05$)。

2.2 BI-RADS 4类乳腺结节评级结果

根据手术或穿刺活检病理结果,在105个BI-RADS 4类乳腺结节中,4A类结节51个,其中良性结节48个,恶性结节3个;4B类结节22个,其中良性结节8个,恶性结节14个;4C类结节32个,其中良性结节2个,恶性结节30个。根据ROC曲线分析,使用常规超声BI-RADS分类系统预测BI-RADS 4类乳腺结节良恶性的AUC值为0.891(95%CI: 0.844~0.957),显示出较高的预测准确性。

2.3 SWE超声参数及诊断效能

良性组和恶性组在Emin、Shell1.0 Emin、Shell2.0 Emax、Shell2.0 Emin、Shell3.0 Emax、Shell3.0 Emin、Shell4.0 Emin、Shell5.0 Emax及Shell5.0 Emin等超声参数上存在显著差异(P 均 < 0.05 ,表1),表明这些参数在乳腺结节良恶性鉴别中具有重要意义。ROC曲线分析发现,Shell2.0 Emax的诊断效能最高,当截断值设定为89.48 kPa时,其预测BI-RADS 4类乳腺结节良恶性的AUC值为0.709(95%CI: 0.609~0.810),灵敏度为53.20%,特异度达84.50%(表2)。

2.4 VE超声参数及诊断效能

恶性组与良性组在Vmean、Vmin、Shell1.0 Vmax、Shell1.0 Vsd、Shell2.0 Vmax、Shell2.0 Vsd、Shell3.0 Vmax、Shell3.0 Vsd、Shell4.0 Vmax、Shell4.0 Vsd、Shell5.0 Vmax及Shell5.0 Vsd等超声参数上存在显著差异(P 均 < 0.05 ,表3)。ROC曲线分析发现Shell3.0 Vmax的诊断价值最为突出。在截断值为5.77 Pa·s时,它对BI-RADS 4类乳腺结节良恶性的预测AUC达到了0.750(95%CI: 0.655~0.845),灵敏度为70.21%,特异度为72.41%(表4)。

2.5 SWE与VE最佳指标联合BI-RADS分类对预测BI-RADS 4类乳腺结节良恶性的诊断效能

ROC曲线分析显示,Shell2.0 Emax与Shell3.0 Vmax联合常规超声BI-RADS分类预测BI-RADS 4类乳腺结节良恶性AUC为0.941(95%CI: 0.889~0.992),灵敏度为93.60%,特异度为93.10%;DeLong检验提示,三者联合应用与BI-RADS、Shell3.0 Vmax、Shell2.0 Emax、Shell3.0 Vmax+Shell2.0 Emax比较,差异均有统计学意义($P < 0.05$,图1,表5)。三者联合应用诊断效能最佳。

表1 良性组和恶性组SWE超声参数比较

Table 1 Comparison of SWE ultrasound parameters between the benign and malignant groups (kPa)

Ultrasonic parameter	Benign group(n=58)	Malignant group(n=47)	P
E _{max} [<i>M</i> (<i>P</i> ₂₅ , <i>P</i> ₇₅)]	49.65(36.58, 63.25)	57.68(36.57, 77.10)	0.250
E _{mean} [<i>M</i> (<i>P</i> ₂₅ , <i>P</i> ₇₅)]	19.40(16.16, 24.03)	17.33(13.18, 22.40)	0.100
E _{min} [<i>M</i> (<i>P</i> ₂₅ , <i>P</i> ₇₅)]	6.30(4.22, 9.07)	3.95(2.95, 5.56)	0.001
E _{sd} [<i>M</i> (<i>P</i> ₂₅ , <i>P</i> ₇₅)]	7.54(5.02, 10.23)	7.39(5.70, 10.78)	0.369
Shell1.0 E _{max} [<i>M</i> (<i>P</i> ₂₅ , <i>P</i> ₇₅)]	57.41(39.83, 69.98)	63.99(39.04, 86.20)	0.140
Shell1.0 E _{mean} ($\bar{x} \pm s$)	22.04 ± 8.25	22.86 ± 10.34	0.880
Shell1.0 E _{min} [<i>M</i> (<i>P</i> ₂₅ , <i>P</i> ₇₅)]	7.10(3.91, 9.72)	4.79(2.99, 7.36)	0.020
Shell1.0 E _{sd} [<i>M</i> (<i>P</i> ₂₅ , <i>P</i> ₇₅)]	10.40(6.55, 13.71)	10.44(6.41, 15.78)	0.569
Shell2.0 E _{max} ($\bar{x} \pm s$)	66.25 ± 24.14	98.91 ± 43.29	< 0.001
Shell2.0 E _{mean} ($\bar{x} \pm s$)	21.38 ± 7.92	23.09 ± 9.90	0.710
Shell2.0 E _{min} [<i>M</i> (<i>P</i> ₂₅ , <i>P</i> ₇₅)]	5.52(2.68, 7.13)	3.25(2.40, 5.17)	0.010
Shell2.0 E _{sd} ($\bar{x} \pm s$)	10.77 ± 4.95	13.17 ± 8.51	0.323
Shell3.0 E _{max} ($\bar{x} \pm s$)	64.84 ± 27.59	82.81 ± 44.92	0.013
Shell3.0 E _{mean} ($\bar{x} \pm s$)	20.44 ± 7.60	22.73 ± 9.29	0.400
Shell3.0 E _{min} ($\bar{x} \pm s$)	4.78 ± 2.32	3.32 ± 2.08	0.002
Shell3.0 E _{sd} ($\bar{x} \pm s$)	10.71 ± 4.79	13.11 ± 8.28	0.305
Shell4.0 E _{max} ($\bar{x} \pm s$)	66.88 ± 27.40	85.70 ± 43.81	0.080
Shell4.0 E _{mean} ($\bar{x} \pm s$)	19.61 ± 7.29	22.05 ± 8.74	0.280
Shell4.0 E _{min} ($\bar{x} \pm s$)	4.01 ± 2.03	3.06 ± 1.94	0.020
Shell4.0 E _{sd} [<i>M</i> (<i>P</i> ₂₅ , <i>P</i> ₇₅)]	10.55(6.93, 14.58)	10.82(6.98, 18.10)	0.270
Shell5.0 E _{max} ($\bar{x} \pm s$)	68.11 ± 26.41	89.12 ± 43.33	0.030
Shell5.0 E _{mean} ($\bar{x} \pm s$)	18.96 ± 7.01	21.26 ± 8.21	0.220
Shell5.0 E _{min} [<i>M</i> (<i>P</i> ₂₅ , <i>P</i> ₇₅)]	3.60(2.40, 4.68)	2.42(1.42, 4.21)	0.020
Shell5.0 E _{sd} [<i>M</i> (<i>P</i> ₂₅ , <i>P</i> ₇₅)]	10.50(7.06, 14.81)	10.63(7.19, 16.92)	0.242

表2 SWE超声参数诊断效能比较

Table 2 Comparison of diagnostic efficacy of SWE ultrasound parameters

Ultrasonic parameter	Cut-off(kPa)	Sensitivity(%)	Specificity(%)	AUC(95%CI)
E _{min}	6.18	17.00	48.30	0.318(0.215-0.422)
Shell1.0 E _{min}	6.68	25.50	44.80	0.363(0.257-0.469)
Shell2.0 E _{max}	89.48	53.20	84.50	0.709(0.609-0.810)
Shell2.0 E _{min}	5.32	23.40	41.40	0.357(0.250-0.465)
Shell3.0 E _{max}	103.48	29.80	93.10	0.591(0.480-0.702)
Shell3.0 E _{min}	5.56	10.60	58.60	0.328(0.225-0.431)
Shell4.0 E _{min}	3.73	27.70	48.30	0.364(0.257-0.470)
Shell5.0 E _{max}	104.30	34.00	93.10	0.623(0.513-0.733)
Shell5.0 E _{min}	2.47	48.90	24.10	0.366(0.259-0.474)

3 讨论

乳腺癌超过肺癌成为全球最常见的癌症,且发病率逐年升高,预计2070年新发病例可达440万^[10]。与其他国家相比,中国乳腺癌的发病人数与死亡病例最多,分别占全球乳腺癌总数18.4%和17.1%^[11]。常规超声因无创、无辐射、操作简单及不受腺体密度

影响等优势成为乳腺癌筛查的首选影像学方法^[12]。美国放射学会发布的常规超声BI-RADS分类^[9]通过观察乳腺病变的形态、边缘特征、回声模式、钙化、后方特征及血流情况等特征综合评估其恶性程度。乳腺恶性结节与良性结节在常规超声图像上存在部分交叉重叠表现,仅凭常规超声评估BI-RADS 4类乳腺结节,易导致漏诊与误诊,进而增加

表3 良性组和恶性组VE超声参数比较

Table 3 Comparison of VE ultrasound parameters the between the benign and malignant groups (Pa·s)

Ultrasonic parameter	Benign group(n=58)	Malignant group(n=47)	P
Vmax[M(P ₂₅ ,P ₇₅)]	4.44(3.65,5.63)	4.50(3.65,6.86)	0.402
Vmean($\bar{x} \pm s$)	1.74 ± 0.60	1.25 ± 0.62	< 0.001
Vmin[M(P ₂₅ ,P ₇₅)]	0.26(0.10,0.41)	0.15(0.10,0.24)	0.012
Vsd[M(P ₂₅ ,P ₇₅)]	0.73(0.49,0.86)	0.64(0.50,0.96)	0.899
Shell1.0 Vmax($\bar{x} \pm s$)	4.63 ± 1.92	6.34 ± 2.93	0.001
Shell1.0 Vmean[M(P ₂₅ ,P ₇₅)]	1.77(1.41,2.10)	1.56(0.92,1.96)	0.146
Shell1.0 Vmin[M(P ₂₅ ,P ₇₅)]	0.16(0.10,0.43)	0.14(0.10,0.30)	0.167
Shell1.0 Vsd[M(P ₂₅ ,P ₇₅)]	0.57(0.82,1.08)	1.00(0.64,1.41)	0.048
Shell2.0 Vmax($\bar{x} \pm s$)	4.79 ± 1.89	7.21 ± 3.14	< 0.001
Shell2.0 Vmean[M(P ₂₅ ,P ₇₅)]	1.66(1.30,2.01)	1.56(1.06,2.09)	0.5731
Shell2.0 Vmin[M(P ₂₅ ,P ₇₅)]	0.13(0.04,0.27)	0.10(0.01,0.20)	0.058
Shell2.0 Vsd[M(P ₂₅ ,P ₇₅)]	0.84(0.61,1.06)	1.07(0.69,1.56)	0.004
Shell3.0 Vmax($\bar{x} \pm s$)	4.99 ± 1.88	7.53 ± 3.07	< 0.001
Shell3.0 Vmean[M(P ₂₅ ,P ₇₅)]	1.51(1.23,1.86)	1.52(1.10,1.94)	0.991
Shell3.0 Vmin[M(P ₂₅ ,P ₇₅)]	0.04(0.01,0.12)	0.01(0.01,0.13)	0.092
Shell3.0 Vsd[M(P ₂₅ ,P ₇₅)]	0.87(0.60,1.04)	1.04(0.75,1.56)	0.002
Shell4.0 Vmax($\bar{x} \pm s$)	5.37 ± 2.08	7.76 ± 2.97	< 0.001
Shell4.0 Vmean[M(P ₂₅ ,P ₇₅)]	1.53(1.13,1.75)	1.40(1.09,1.91)	0.839
Shell4.0 Vmin[M(P ₂₅ ,P ₇₅)]	0.02(0.01,0.73)	0.01(0.01,0.08)	0.066
Shell4.0 Vsd[M(P ₂₅ ,P ₇₅)]	0.90(0.59,1.03)	1.06(0.73,1.49)	0.001
Shell5.0 Vmax($\bar{x} \pm s$)	5.53 ± 2.18	7.81 ± 2.96	< 0.001
Shell5.0 Vmean($\bar{x} \pm s$)	1.41 ± 0.46	1.47 ± 0.48	0.506
Shell5.0 Vmin[M(P ₂₅ ,P ₇₅)]	0.01(0.01,0.03)	0.01(0.01,0.02)	0.062
Shell5.0 Vsd[M(P ₂₅ ,P ₇₅)]	0.92(0.59,1.11)	1.00(0.76,1.41)	0.003

表4 VE超声参数诊断效能比较

Table 4 Comparison of diagnostic efficacy of VE ultrasound parameters

Ultrasonic parameters	Cut-off(Pa·s)	Sensitivity(%)	Specificity(%)	AUC(95%CI)
Vmean	1.15	46.80	13.80	0.272 (0.173-0.371)
Vmin	0.31	4.30	62.10	0.357(0.251-0.463)
Shell1.0 Vmax	5.44	57.40	75.90	0.669(0.563-0.775)
Shell1.0 Vsd	1.30	34.00	89.70	0.612(0.502-0.722)
Shell2.0 Vmax	6.20	61.70	79.31	0.730(0.632-0.829)
Shell2.0 Vsd	1.07	51.06	79.31	0.664(0.559-0.770)
Shell3.0 Vmax	5.77	70.21	72.41	0.750(0.655-0.845)
Shell3.0 Vsd	1.14	46.80	86.20	0.679(0.575-0.783)
Shell4.0 Vmax	6.75	61.70	79.31	0.733(0.637-0.830)
Shell4.0 Vsd	1.16	44.70	86.20	0.685(0.582-0.787)
Shell5.0 Vmax	6.75	61.70	75.86	0.726(0.630-0.823)
Shell5.0 Vsd	1.18	42.60	89.70	0.670(0.566-0.774)

医疗成本,加剧患者心理负担。因此,探索能有效提升BI-RADS 4类乳腺结节诊断准确率,并减少漏诊与误诊的影像学检查方法,仍是临床研究的重点。近年来,SWE技术通过定量评估乳腺病变组织的硬

度,成为常规超声检查诊断乳腺癌的重要补充^[4-6]。但是研究表明,SWE技术将乳腺组织假设为纯弹性介质,忽略了组织的黏弹性反应^[7-8]。引入黏性物理参数的VE技术作为一种崭新的超声技术,在临床

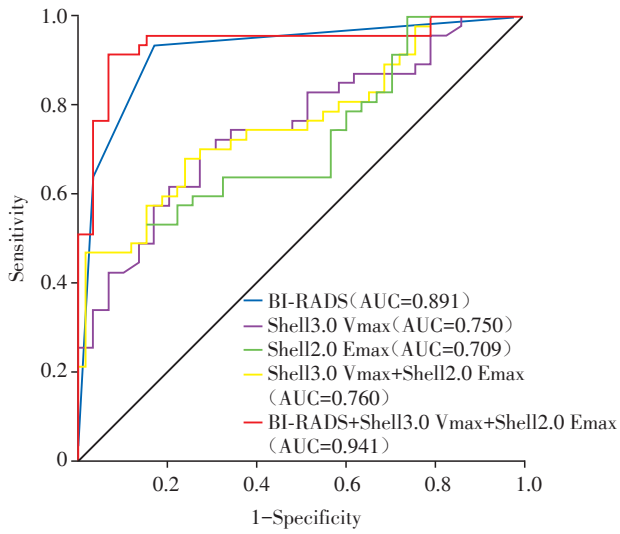


图1 Shell2.0 Emax 与 Shell3.0 Vmax 单独及联合 BI-RADS 分类预测 BI-RADS 4 类乳腺结节良恶性的 ROC 曲线
Figure 1 ROC curve of Shell2.0 Emax and Shell3.0 Vmax alone and in combination with BI-RADS to predict the benign and malignant of BI-RADS 4 breast nodules

上应用起步,本研究通过 VE 联合 SWE 技术期待进一步提升 BI-RADS 4 类乳腺病灶良恶性诊断的灵敏度和特异度。

SWE 技术通过运用外部力量对组织施加压力,根据组织的变形与移位情况生成展示其硬度特征的弹性模量分布图。因乳腺恶性肿瘤组织中的胶原纤维密度及空间排列方向与组织硬度密切相关,SWE 技术在乳腺癌筛查中被广泛使用^[13-14]。本研究 ROC 曲线分析显示,Shell2.0 Emax 诊断价值最高,当截断值为 89.48 kPa 时,其预测 BI-RADS 4 类乳腺结节良恶性的 AUC 为 0.709 (95%CI: 0.609~0.810),灵敏度为 53.20%,特异度为 84.50%。Shell2.0 Emax 诊断价值最高与以往的观点一致^[14-16],但是其截断值与上述研究差异较大,考虑主要原因是研究只入组 BI-RADS 4 类乳腺结节,5 类和 3 类结节未被纳入,数值存在一定的差异。虽 Shell2.0 Emax 预测 BI-RADS 4 类乳腺结节良恶性的特异度高,但灵敏度低,仅为 53.2%,导致假阴性占比增高,易出现漏诊,分析可

表5 SWE 与 VE 最佳指标单独及联合 BI-RADS 分类诊断效能比较

Table 5 Comparison of diagnostic efficacy of SWE and VE best indicators alone and in combination with BI-RADS

Ultrasonic parameter	Sensitivity (%)	Specificity (%)	AUC (95%CI)
BI-RADS	89.50	82.80	0.891 (0.844-0.957)
Shell3.0 Vmax	70.21	72.41	0.750 (0.655-0.845)
Shell2.0 Emax	53.20	84.50	0.709 (0.609-0.810)
Shell3.0 Vmax+Shell2.0 Emax	46.80	98.30	0.760 (0.667-0.854)
BI-RADS+Shell3.0 Vmax+Shell2.0 Emax	93.60	93.10	0.941 (0.889-0.992)

能原因:一方面,乳腺恶性结节内部可能出现液化或坏死等导致组织变软的情况;另一方面,SWE 技术将乳腺假设为纯弹性的介质,可能忽略了其具有黏弹性反应的特点^[7-8],导致硬度评估存在误差。超声检查时,超声波束的辐射力在组织内产生横波,并测量横波的传播速度,而组织中的剪切波速度与频率色散有关,这是由组织黏度引起的^[17]。因此,只从剪切波速度计算有效弹性可能忽略了色散效应造成的偏差。VE 技术引入了黏性物理参数,不仅包含 SWE 模型,还包含组织状态的黏度信息。2018 年 Kumar 等^[7]首次报道乳腺恶性结节本身的剪切黏度大于良性结节,乳腺恶性结节的剪切黏度为 8.22 Pa·s,良性结节仅为 2.83 Pa·s。Li 等^[18]研究认为黏弹性对预测乳腺结节良恶性具有较高的诊断效能,当结节本身黏度最大值为 5.39 Pa·s 时,预测灵敏度为 75.68%,特异度为 68.80%。虽然黏弹性与乳腺癌的相关性已得到部分证实,但是针对

BI-RADS 4 类乳腺结节良恶性的预测方面国内外鲜有报道。本研究结果显示,BI-RADS 4 类乳腺结节良性组和恶性组 Vmean、Vmin、Shell1.0 Vmax、Shell1.0 Vsd、Shell2.0 Vmax、Shell2.0 Vsd、Shell3.0 Vmax、Shell3.0 Vsd、Shell4.0 Vmax、Shell4.0 Vsd、Shell5.0 Vmax 及 Shell5.0 Vsd 超声参数差异均有统计学意义 (P 均 < 0.05),表明 BI-RADS 4 类乳腺结节良恶性与黏度有关,且恶性结节比良性结节黏度更大。分析原因:一方面,可能由于纤维增生反应,使胶原和纤维连接蛋白的密度增加,相关蛋白聚糖分子的密度降低,导致乳腺癌高黏度^[19];另一方面,可能由于乳腺癌的异质性^[20]。本研究 ROC 曲线分析显示,Shell2.0 Vmax、Shell3.0 Vmax、Shell4.0 Vmax 和 Shell5.0 Vmax 具有中等诊断效能,以 Shell3.0 Vmax 诊断价值最高,当截断值为 5.77 Pa·s 时,其预测 BI-RADS 4 类乳腺结节良恶性的 AUC 为 0.750 (95%CI: 0.655~0.845),灵敏度为 70.21%,特异度为

72.41%。与瘤体本身比较,瘤周区域黏度信息更有诊断价值,原因可能在于乳腺恶性肿瘤向周围组织浸润,瘤周区域发生间质反应增生、新生血管形成及淋巴管浸润等变化,引起瘤周组织变硬^[21],这与Kumar等^[7]和Li等^[18]的研究结果不同。本研究瘤周Shell3.0 Vmax的诊断性能最高,对临床判断乳腺结节的性质更具参考意义,与黄淑念^[22]和Jia等^[23]研究结果瘤周2 mm黏度参数诊断价值最佳不一致。分析原因:①本研究将瘤周区域以1.0 mm作为间隔差值,向肿瘤外部做Shell环(1.0~5.0 mm),共设定为5组;②本研究针对BI-RADS 4类乳腺结节良恶性的预测结果可能受到入组结节差异的影响;③样本量较少可能会影响研究结果。本研究结果显示,与SWE技术相比,VE技术的最佳指标虽然特异度略有下降,但灵敏度显著提升,从而降低了漏诊率,进一步证实了VE技术在提高BI-RADS 4类乳腺结节中恶性结节检出率方面的优势。

本研究ROC曲线分析显示,常规超声BI-RADS分类预测BI-RADS 4类乳腺结节良恶性的AUC为0.891(95%CI:0.844~0.957),灵敏度为89.50%,特异度为82.80%,与国内以往的研究结果基本一致^[24-25]。但李易凤等^[26]研究认为BI-RADS分类诊断乳腺结节良恶性的特异度仅为32.7%。结果与其不一致的原因考虑为本研究将BI-RADS 4A类的结节判定为良性。本研究旨在通过联合VE与SWE技术,提升BI-RADS 4类乳腺病灶良恶性诊断的灵敏度和特异度,ROC曲线分析显示,SWE最佳指标(Shell2.0 Emax)与VE最佳指标(Shell3.0 Vmax)联合BI-RADS分类在预测BI-RADS 4类乳腺结节良恶性方面表现出色,AUC达到0.941(95%CI:0.889~0.992),灵敏度为93.60%,特异度为93.10%,三者联合应用诊断效能最佳,差异具有统计学意义($P < 0.05$)。联合诊断显著降低了乳腺BI-RADS 4类病变的假阴性率和假阳性率,进而减少了乳腺良恶性病变的漏诊和误诊,避免了不必要的穿刺活检,为乳腺结节的临床诊疗提供了重要的参考依据。但是本研究联合应用对BI-RADS 4类乳腺结节进行良恶性诊断时,也出现了漏诊和误诊的病例。①2例导管内原位癌漏诊,分析原因可能为体积较小,位置较深,生长于导管内未出现周围组织浸润等恶性特征;②1例导管内乳头状瘤误诊,原因可能为瘤体内出血,其周围形成纤维化,表现为假性浸润等恶性特征;③1例乳腺炎性病变误诊,原因可能为炎性细胞渗出和周围组织的水肿等。

本研究的局限性:①本研究为回顾性设计,且

样本量有限,因此,未来亟需开展大规模、多中心的前瞻性研究以进一步验证结论。②SWE与VE技术依赖于人工勾勒乳腺病变轮廓,这一过程中可能存在一定的人为误差。③BI-RADS分类的评估过程具有一定的主观判断成分。本研究的优势:对乳腺病变瘤周区域进行了细致分组,以1.0 mm为间隔,自1.0 mm至5.0 mm共设置5组Shell环,分组方法更为全面且精细。

综上,VE瘤周超声参数预测BI-RADS 4类乳腺结节良恶性具有较高的诊断价值,VE、SWE技术联合常规超声BI-RADS分类对乳腺BI-RADS 4类结节良恶性的诊断效能最佳,具有简便、无创和可重复的优点,可早期为临床乳腺结节的决策提供有效的影像学依据。

利益冲突声明:

所有作者声明没有利益冲突。

Conflict of Interests:

The authors declare that there are no conflict of interests.

作者贡献声明:

周锋盛和袁琳起草和撰写文稿,获取、分析、解释本研究的数据;浦浙宁、吴越、张雨、杨树东和秦安分析解释本研究的数据,对稿件内容进行了修改;张平洋设计本研究的方案,对稿件的重要内容进行了修改。

Author's Contributions:

ZHOU Fengsheng and YUAN Lin drafted and wrote the manuscript, obtained, analyzed and interpreted the data of this study. PU Zhening, WU Yue, ZHANG Yu, YANG Shudong, and QIN An analyzed and interpreted the data of this study, and revised the content of the manuscript. ZHANG Pingyang designed the research and made significant revisions to the manuscript.

[参考文献]

- [1] BRAY F, LAVERSANNE M, SUNG H, et al. Global cancer statistics 2022: GLOBOCAN estimates of incidence and mortality worldwide for 36 cancers in 185 countries[J]. CA Cancer J Clin, 2024, 74(3): 229-263
- [2] ZHENG F Y, YAN L X, HUANG B J, et al. Comparison of retraction phenomenon and BI-RADS-US descriptors in differentiating benign and malignant breast masses using an automated breast volume scanner[J]. Eur J Radiol, 2015, 84(11): 2123-2129
- [3] SĂFTOIU A, GILJA O H, SIDHU P S, et al. The EF-SUMB guidelines and recommendations for the clinical practice of elastography in non-hepatic applications: update 2018[J]. Ultraschall Med, 2019, 40(4): 425-453
- [4] PARK S Y, KANG B J. Combination of shear-wave elastography with ultrasonography for detection of breast

- cancer and reduction of unnecessary biopsies: a systematic review and meta-analysis[J]. *Ultrasonography*, 2021, 40(3):318-332
- [5] GOLATTA M, PFOB A, BÜSCH C, et al. The potential of shear wave elastography to reduce unnecessary biopsies in breast cancer diagnosis: an international, diagnostic, multicenter trial[J]. *Ultraschall Med*, 2023, 44(2): 162-168
- [6] 戚敏, 王颖彦, 沈会明, 等. 剪切波弹性成像与超声造影联合评分对乳腺病灶定性诊断的临床研究[J]. *南京医科大学学报(自然科学版)*, 2021, 41(2): 258-261, 285
- QI M, WANG Y Y, SHEN H M, et al. Clinical study on the diagnosis of breast lesions by shear wave elastography combined with contrast-enhanced ultrasound[J]. *Journal of Nanjing Medical University (Natural Sciences)*, 2021, 41(2):258-261, 285
- [7] KUMAR V, DENIS M, GREGORY A, et al. Viscoelastic parameters as discriminators of breast masses: initial human study results [J]. *PLoS One*, 2018, 13(10): e0205717
- [8] KOBAYASHI Y, OKAMURA N, TSUKUNE M, et al. Non-minimum phase viscoelastic properties of soft biological tissues [J]. *J Mech Behav Biomed Mater*, 2020, 110: 103795
- [9] American College of Radiology (ACR). Breast imaging reporting and data system (BI-RADS). 5th ed[M]. Reston VA: American College of Radiology, 2013
- [10] SOERJOMATARAM I, BRAY F. Planning for tomorrow: global cancer incidence and the role of prevention 2020-2070[J]. *Nat Rev Clin Oncol*, 2021, 18(10): 663-672
- [11] 雷少元, 郑荣寿, 张思维, 等. 乳腺癌发病率和死亡率的全球模式: 一项基于人群的2000—2020年肿瘤登记数据分析研究[J]. *癌症*, 2022, 41(7): 324-335
- LEI S Y, ZHENG R S, ZHANG S W, et al. Global patterns of breast cancer incidence and mortality: a population-based analysis of cancer registry data from 2000-2020[J]. *Chinese Journal of Cancer*, 2022, 41(7): 324-335
- [12] 朱美娣, 许紫鹏, 华玲玲, 等. 基于B超特征构建外侧象限乳腺癌腋窝淋巴结转移列线图预测模型[J]. *南京医科大学学报(自然科学版)*, 2025, 45(1): 13-21
- ZHU M D, XU Z P, HUA L L, et al. Development a nomogram predictive model for axillary lymph node metastasis in lateral quadrant breast cancer based on B-ultrasound features[J]. *Journal of Nanjing Medical University (Natural Sciences)*, 2025, 45(1): 13-21
- [13] 智文祥, 周瑾, 刘晔旭, 等. 剪切波弹性成像评估不同大小人源性裸鼠三阴性乳腺癌弹性特征与临床病理的关系[J]. *中华超声影像学杂志*, 2021, 30(4): 346-350
- ZHI W X, ZHOU J, LIU C X, et al. Assessment of different size tumor stiffness characteristic with shear wave elastography in a triple-negative human breast cancer implantation model[J]. *Chinese Journal of Ultrasonography*, 2021, 30(4): 346-350
- [14] 孟飞逸, 焦兰兰, 范晨晨, 等. 剪切波弹性成像在乳腺肿块良恶性鉴别及腋窝淋巴结转移预测中的临床价值[J]. *临床超声医学杂志*, 2025, 27(5): 400-407
- MENG F Y, JIAO L L, FAN C C, et al. Clinical value of shear wave elastography in the differentiation of benign and malignant breast masses and prediction of lymph node metastasis [J]. *Journal of Clinical Ultrasound in Medicine*, 2025, 27(5): 400-407
- [15] BERG W A, MENDELSON E B, COSGROVE D O, et al. Quantitative maximum shear - wave stiffness of breast masses as a predictor of histopathologic severity[J]. *AJR Am J Roentgenol*, 2015, 205(2): 448-455
- [16] 王华, 朱岩冰, 丁赟洁, 等. 剪切波弹性成像技术定量评估肿块周围组织硬度对乳腺良恶性肿瘤鉴别诊断的价值[J]. *现代肿瘤医学*, 2023, 31(6): 1099-1103
- WANG H, ZHU Y B, DING Y J, et al. The value of shear wave elastography in quantitative assessment of tissue hardness around mass in the diagnosis of benign and malignant breast tumors[J]. *Journal of Modern Oncology*, 2023, 31(6): 1099-1103
- [17] CHEN S G, SANCHEZ W, CALLSTROM M R, et al. Assessment of liver viscoelasticity by using shear waves induced by ultrasound radiation force [J]. *Radiology*, 2013, 266(3): 964-970
- [18] LI W Y, JIANG J, CAO J Y, et al. The value of ultrasound viscosity imaging in preoperative differential diagnosis between malignant and benign breast lesions: preliminary clinical applications [J]. *Clin Hemorheol Microcirc*, 2025, 89(1): 111-122
- [19] SRIDHAR M, INSANA M F. Ultrasonic measurements of breast viscoelasticity[J]. *Med Phys*, 2007, 34(12): 4757-4767
- [20] ZHANG H M, GUO Y, ZHOU Y, et al. Fluidity and elasticity form a concise set of viscoelastic biomarkers for breast cancer diagnosis based on Kelvin-Voigt fractional derivative modeling [J]. *Biomech Model Mechanobiol*, 2020, 19(6): 2163-2177
- [21] BAI X F, WANG Y Y, SONG R X, et al. Ultrasound and clinicopathological characteristics of breast cancer for predicting axillary lymph node metastasis [J]. *Clin Hemorheol Microcirc*, 2023, 85(2): 147-162

- [22] 黄淑念. 黏弹性及剪切波弹性定量参数联合BI-RADS分类量化评分诊断乳腺结节的价值探讨[D]. 百色: 右江民族医学院, 2024
HUANG S N. The value of viscoelastic and shear-wave elastic parameter combined with BI - RADS quantified score in the diagnosis of breast nodules[D]. Baise: Youjiang Medical College for Nationalities, 2024
- [23] JIA W R, XIA S J, JIA X H, et al. Ultrasound viscosity imaging in breast lesions: a multicenter prospective study[J]. *Acad Radiol*, 2024, 31(9): 3499-3510
- [24] 梁汝娜, 张瑾晖, 井佳瑜, 等. 基于常规超声与超声造影特征构建列线图对乳腺BI-RADS 4类病变风险预测的研究[J]. *中国超声医学杂志*, 2025, 41(2): 136-140
LI R N, ZHANG J H, JIN J Y, et al. Study on risk prediction of BI-RADS 4 breast lesions by constructing a nomogram model based on conventional ultrasound and contrast-enhanced ultrasound features [J]. *Chinese Journal of Ultrasound in Medicine*, 2025, 41(2): 136-140
- [25] 曹钟毓, 周 鸿, 翟 蓓, 等. 剪切波弹性成像联合超微血管成像对BI-RADS 4类乳腺结节的诊断价值[J]. *成都医学院学报*, 2024, 19(6): 958-961
CAO Z Y, ZHOU H, ZHAI B, et al. Value of shear wave elastography combined with superb microvascular imaging in the diagnosis of B-RADS4 breast nodule[J]. *Journal of Chengdu Medical College*, 2024, 19(6): 958-961
- [26] 李易凤, 陈 武, 刘晓芳, 等. 剪切波弹性成像在乳腺结节BI-RADS 3、4a类中的应用价值[J]. *中国超声医学杂志*, 2020, 36(7): 613-616
LI Y F, CHEN W, LIU X F, et al. Application value of shear-wave elastography in category BI-RADS 3 and 4a of breast lesions[J]. *Chinese Journal of Ultrasound in Medicine*, 2020, 36(7): 613-616
- [收稿日期] 2025-08-06
(本文编辑: 蒋 莉)

(上接第1545页)

- against triple-negative breast cancer[J]. *Chem Biol Interact*, 2023, 369: 110260
- [14] ZHU J R, WANG L, NIE X Y, et al. RBMS3-loss impedes TRIM21-induced ubiquitination of ANGPT2 in an RNA-independent manner and drives sorafenib resistance in hepatocellular carcinoma[J]. *Oncogene*, 2025, 44(21): 1620-1633
- [15] ZHANG Q S, HAN S Q, ZHANG X Y, et al. Metformin enhances PD-L1 inhibitor efficacy in ovarian cancer by modulating the immune microenvironment and RBMS3 expression[J]. *FASEB J*, 2025, 39(11): e70705
- [16] RUAN X L, LIU Y H, WANG P, et al. RBMS3-induced circHECTD1 encoded a novel protein to suppress the vasculogenic mimicry formation in glioblastoma multiforme[J]. *Cell Death Dis*, 2023, 14(11): 745
- [17] ENGELAND K. Cell cycle regulation: p53-p21-RB signaling[J]. *Cell Death Differ*, 2022, 29(5): 946-960
- [18] TICLI G, CAZZALINI O, STIVALA L A, et al. Revisiting the function of p21^{CDKN1A} in DNA repair: the influence of protein interactions and stability[J]. *Int J Mol Sci*, 2022, 23(13): 7058
- [19] THANGAVELU L, ALTAMIMI A S A, GHABOURA N, et al. Targeting the p53-p21 axis in liver cancer: linking cellular senescence to tumor suppression and progression[J]. *Pathol Res Pract*, 2024, 263: 155652
- [20] WAGA S, HANNON G J, BEACH D, et al. The p21 inhibitor of cyclin-dependent kinases controls DNA replication by interaction with PCNA[J]. *Nature*, 1994, 369(6481): 574-578
- [21] ZHANG C, WANG S F, LU X Q, et al. POP1 Facilitates proliferation in triple-negative breast cancer via m6A-dependent degradation of CDKN1A mRNA[J]. *Research (Wash D C)*, 2024, 7: 0472
- [22] 奚佩雯, 胡 玥, 张 旭, 等. RBM7在乳腺癌细胞BT474中的表达及其与P21的关系[J]. *南京医科大学学报(自然科学版)*, 2020, 40(2): 160-165
XI P W, HU Y, ZHANG X, et al. Expression of RBM7 in breast cancer cell line BT474 and its relationship with P21[J]. *Journal of Nanjing Medical University (Natural Sciences)*, 2020, 40(2): 160-165
- [23] XI P W, ZHANG X, ZHU L, et al. Oncogenic action of the exosome cofactor RBM7 by stabilization of CDK1 mRNA in breast cancer[J]. *NPJ Breast Cancer*, 2020, 6: 58
- [24] XU F, XIA T, XU Q T, et al. RBMS2 chemosensitizes breast cancer cells to doxorubicin by regulating BMF expression[J]. *Int J Biol Sci*, 2022, 18(4): 1724-1736
- [25] XIA T, DAI X Y, SANG M Y, et al. IGF₂BP₂ drives cell cycle progression in triple-negative breast cancer by recruiting EIF4A1 to promote the m6A-modified CDK6 translation initiation process[J]. *Adv Sci (Weinh)*, 2024, 11(1): e2305142
- [收稿日期] 2025-07-27
(本文编辑: 陈汐敏)